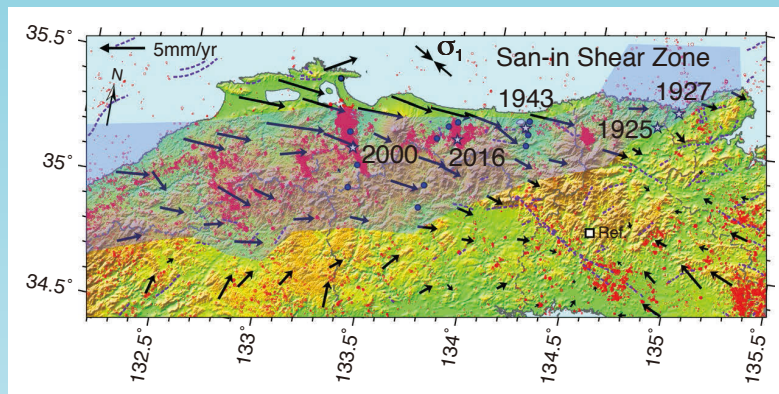


Earth, Planets and Space

Crustal Dynamics: Unified Understanding of Geodynamics
Processes at Different Time and Length Scales



Society of Geomagnetism and Earth, Planetary and Space Sciences (SGEPSS)
The Seismological Society of Japan
The Volcanological Society of Japan
The Geodetic Society of Japan
The Japanese Society for Planetary Sciences



Springer Open

Editorial Board (September 2019)

Editor-in-Chief

Yasuo Ogawa, Tokyo Institute of Technology, Japan

Vice Editors-in-Chief

Masato Furuya, Hokkaido University, Japan
Solid Earth Science

Nozomu Nishitani, Nagoya University, Japan
Space Science

Editors

Valerio Acocella
Ryosuke Ando
Kimiyouki Asano
Nanan Balan
Paul Bedrosian
Phil Cummins
Hao Dong
Koji Fukuma
Shin-Chan Han
James Hickey
Thomas Hobiger
Hauke Hussmann
Takeo Ito
Art Jolly
Tomokazu Kobayashi
Attila Komjathy

Alexey Kuvshinov
Juanjo Ledo
Huixin Liu
Yohei Miyake
Mitsuhiro Nakagawa
Junichi Nakajima
Haruhisa Nakamichi
Yasuhito Narita
Takuya Nishimura
Takaaki Noguchi
Masahito Nose
Makiko Ohtake
Keiji Ohtsuki
Kyoko Okino
Duggirala Pallamraju
Severine Rosat

Akinori Saito
Tatsuhiko Saito
David Shelly
Hiroko Sugioka
Benoit Taisne
Sunny Tam
Yoshiyuki Tanaka
Yanbin Wang
Yih-Min Wu
Chuang Xuan
Takuji Yamada
Mare Yamamoto
Tadashi Yamasaki
Tatsuhiko Yokoyama
Kazunori Yoshizawa

Advisory Board

Benjamin Fong Chao
Bernard Chouet
Yoshimori Honkura
Toshihiko Iyemori

Hiroo Kanamori
Jun'ichiro Kawaguchi
Takafumi Matsui
Hitoshi Mizutani

Toshitaka Tsuda
Zhongliang Wu
Kiyoshi Yomogida

Journal Scope

Earth, Planets and Space (EPS) is the official journal of the Society of Geomagnetism and Earth, Planetary and Space Sciences, The Seismological Society of Japan, The Volcanological Society of Japan, The Geodetic Society of Japan, and The Japanese Society for Planetary Sciences.

EPS is a peer-reviewed, open-access journal published under SpringerOpen. It is an international journal covering scientific articles in the entire field of earth and planetary sciences, particularly geomagnetism, aeronomy, space science, seismology, volcanology, geodesy, and planetary science. EPS also welcomes articles in new and interdisciplinary subjects, and technical reports on instrumentation and software.

The journal was launched in 1998 and has since published over 3000 articles. All of them are available for free on SpringerLink:

<http://link.springer.com/journal/40623>

More information about the journal, its article collections, and the submission process is available on the journal homepage:

<http://earth-planets-space.springeropen.com>

Submit your next research article to Earth, Planets and Space via:

<https://www.editorialmanager.com/eps>

Yours sincerely,

Prof. Yasuo Ogawa
Editor-in-Chief, *Earth, Planets and Space*
editor-in-chief@earth-planets-space.org

PREFACE

Open Access



Crustal dynamics: unified understanding of geodynamic processes at different time and length scales

Yoshihisa Iio^{1*}, Richard H. Sibson², Toru Takeshita³, Takeshi Sagiya⁴, Bunichiro Shibazaki⁵ and Junichi Nakajima⁶

Keywords: Crustal dynamics, Tohoku-oki earthquake, Stress, Strength, Deformation, Fault zone, Friction, Rheology, Crustal fluid, Materials science

The 2011 Tohoku-oki earthquake occurred on an unexpected scale, which made us realize that the generation mechanisms of earthquakes are poorly understood. To provide a unified view of the geodynamic processes including earthquake generation processes in the Japanese arc–trench system, it is necessary to clarify the absolute values of crustal stresses, the stress–strain field, and the basic properties of the island arc crust and mantle, in particular, those of fault zones. This special issue includes 22 papers, and they are divided into several categories: (1) crustal stress and overpressured fluids, (2) stress and rupture heterogeneity, (3) large-scale deformation in the Japanese Island Arc, (4) shear zone detected by Satellite Geodesy, (5) rheology of crustal fault zones, (6) materials science of rock deformation.

Several papers analyzed spatiotemporal changes in crustal stress related to earthquake generation and volcanic eruption and discussed involvement of overpressured fluids in seismogenesis and fault zone properties related to overpressure. Hardebeck (2017) investigated coseismic and postseismic rotations of principal stress axes caused by three $M > 8.8$ subduction megathrust ruptures. The largest coseismic stress rotations occur just above the Moho depth of the overriding plate where large continuous slip patches appear (from seismological studies) to coincide with areas of intense fluid overpressuring inferred to promote near-complete shear stress

drop. Modeling the full spatial distribution of static stress changes during the mainshock is probably needed to account for the spatial complexity of coseismic stress rotations. Otsubo et al. (2018) employed the multiple inverse method (MIM) to demonstrate significant variations in the normal faulting stress state around Iwaki City, Japan, over a period of a few years prior to the 2011 Mw 9.0 Tohoku megathrust earthquake. Such variations in stress state require a low differential stress state which they attribute to overpressured fluids in the focal regions. Terakawa (2017) analyzed slip plane diversity within microearthquake swarms around Mt. Ontake stratovolcano to make the case that local swarm activity is driven by regions where pore fluids are overpressured by 10–30 MPa. Matsumoto and Shigematsu (2018) reported measurements of fault zone permeability from borehole intercepts along the Median Tectonic Line (MTL) in Mie Prefecture, SW Japan, finding values more than 100–700 times the permeability of the surrounding protolith assemblage of crystalline rocks. While reported permeabilities ($5 \times 10^{-16} \text{ m}^2 > k > 3 \times 10^{-19} \text{ m}^2$) are generally too high to contain overpressured fault fluids at depth, it has to be kept in mind that the measurements were made under low confining pressure at depths of only a few hundred meters. Sibson (2017) advanced the hypothesis that the local attainment of the tensile overpressure state ($P_f > \sigma_3$) is associated with the formation and activation of fault–fracture meshes distributed throughout tabular volumes. Except in the near surface this generally requires near-lithostatic fluid overpressures. Interlinkage of shear fractures with fluid-saturated extension fractures

*Correspondence: iio@rcep.dpri.kyoto-u.ac.jp

¹ Research Center for Earthquake Prediction, Disaster Prevention Research Institute, Kyoto University, Uji, Japan

Full list of author information is available at the end of the article

slows slip transfer, allowing such mesh structures to function as rheological units incorporating viscous dashpots capable of giving rise to a variety of anomalous slow-slip phenomena.

Full understanding of crustal dynamics requires clarification of stress and strength heterogeneities, and rupture heterogeneity. Yukutake and Iio (2017) conducted a precise analysis of hypocenters and focal mechanisms of upper crustal aftershocks from the 2000 Mw 6.6 Western Tottori, Japan, earthquake which involved predominantly sinistral strike-slip along a NNW–SSE fault structure disrupted by a conjugate set of dextral cross-faults. Aftershocks around the mainshock rupture plane occur within a tabular zone 1.0–1.5 km thick, significantly broader than the likely damage zone, with diverse mechanisms. The aftershocks apparently represent rupture of fractures surrounding the mainshock rupture rather than reshear of the primary rupture, caused by stress changes arising from heterogeneous slip distribution along the mainshock rupture. Iio et al. (2017) employed a high-density seismological network in western Nagano Prefecture. Focal mechanisms were inverted to show that the crustal stress field can generally be regarded as uniform at a scale of 1 km throughout the study region, but that strength is heterogeneous, varying over comparatively short distances (~100 m). Ando et al. (2017) analyzed complex patterns in the wave radiation and surface displacement of the 2014 Mw 6.2 northern Nagano earthquake sequence which involved predominantly reverse slip on an irregularly segmented rupture. Observations include foreshock occurrence, large differences between the first-motion focal mechanisms and the CMT, and along-strike variations in surface displacement. Aftershocks reveal a more complex geometry in the northern half of the focal area, correlated with along-strike variation of fault activity and maturity. Dynamic rupture simulations took account of the observationally determined regional stress field and fault geometry. The observed complexity is explained as the effect of non-planar fault geometry with a number of branch faults and bends. Maeda et al. (2018) explored the spatial relationship between upper crustal structure and seismicity in the Kii Peninsula of southwest Japan, where the stress field and the predominant focal mechanism change with depth. They attribute this stress heterogeneity to localized thermal stress from a buried heat source in the lower crust.

Deformation occurs in response to stress and/or stress changes, and it reflects material properties where the deformation occurs. Thus, it is crucial to measure deformation and/or deformation rate in the Japanese Island Arc. Sueoka et al. (2017) employed (U-Th)/He thermochronometric analyses across southern Tohoku in the Japan arc to reconstruct the long-term uplift and

denudation history of the region. Distinct morphostructural provinces defined by apatite He ages are distinguished, the Abukuma Mountains on the fore-arc side (64.3–49.6 Ma), the Ou Backbone Range along the volcanic front (11.4–1.5 Ma), and the Asahi Mountains on the back-arc side (<10 Ma). Denudation rates of <0.1 mm/year are estimated for the Abukuma Mountains, 0.1–1.0 mm/year for the Ou Backbone range, and 0.1–0.3 mm/year for the Asahi Mountains. These techniques could be extended across other segments of the arc, but possible thermal effects of magmatism need to be carefully considered.

Finer-scale deformation is estimated by Satellite Geodesy along major fault zones in Japan. Nishimura and Takada (2017) used GNSS velocity data to define the San-in dextral shear zone with a width of c. 50 km accommodating c. 5 mm/year of dextral shearing along the northern coastline of southwest Japan. Major recent earthquake ruptures appear to follow anticipated trajectories of conjugate Riedel shears within the shear zone. Takada et al. (2018) employed Satellite Geodesy (InSAR and GNSS) to define a sharp velocity gradient across the Ushikubi fault within the dextral Atotsugawa fault system in central Japan. Analysis of InSAR data shows interseismic deformation to be spatially heterogeneous within the strain concentration zone.

Rheology of large-scale crustal fault zones is essential in the crustal dynamics, because it can control deformation in the whole crust in island arcs. Nakajima and Matsuzawa (2017) used high-quality waveform data from a dense seismic network to explore the three-dimensional P-wave attenuation structure at depth along the Niigata–Kobe Tectonic Zone (NKTZ) in central Japan. The study confirms spatial relationships between attenuation structures and surface deformation along the NKTZ. Anelastically weakened lower crust west of the Itoigawa–Shizuoka Tectonic Line (ISTL) promotes surface contraction over a region about 100 km wide while anelastic deformation in the thick, shallow sedimentary basin east of the ISTL restricts surface deformation to a narrow region (25–40 km). These observations account qualitatively for regional variations in the width of the high-strain-rate zone across the ISTL, placing constraints on the character of deformation in the subsurface. Dojo and Hiramatsu (2017) used the spatial distribution of coda Q from the analysis of waveform data to investigate a high-strain-rate region in the northeastern part of the Niigata–Kobe Tectonic Zone (NKTZ). Coda Q in the 2–3 Hz frequency band correlates spatially with S wave velocity at 25 km depth, while Coda Q in the 4–8 Hz band correlates with S wave velocity perturbations at 10 km depth. Results indicate that a combination of deformation in the upper crust as well as ductile deformation in the lower

crust may contribute to the high strain rate in the north-eastern NKTZ. Zhang and Sagiya (2017) modeled strain concentration in two dimensions within the lower crust, assuming steady fault sliding in the upper crust and ductile flow in the lower crust according to laboratory-derived power-law rheology with a yield threshold at the brittle–ductile transition. Possible physical mechanisms for strain concentration in the lower crust are investigated including frictional and shear heating, grain size, and power-law creep, taking account also of the role of water in promoting crystal plasticity.

Materials science of rock deformation is fundamental for not only the crustal dynamics but also all the studies in solid earth sciences. Consequently, its progress is crucial for our understanding of crustal dynamics. Fukuda et al. (2018) showed how the addition of small amounts of water to polycrystalline anorthite under high temperature induces a change from distributed fracturing to plastic flow promoting grain-size-sensitive creep in the lower middle crust. Kameda et al. (2017) investigated the alteration and dehydration of subducting oceanic crust, specifically pillow basalts within the Shimanto belt showing how the saponite–chlorite conversion within mixed layer C/S minerals may contribute fluid to plate boundary fault systems with consequent mechanical effects. Kuwatani and Toriumi (2017) employed a new forward modeling technique for analyzing retrogressive hydration reactions. Results indicate that changes in mineral composition are mainly controlled by pressure and temperature, but that changes in mineral modes are controlled by the degree of water infiltration. Matsumura et al. (2017) statistically analyzed two probability density functions to evaluate a microboudin palaeopiezometer applied to stretched tourmaline grains within Archean metacherts from the East Pilbara Terrane in Western Australia. They found that an elastic matrix model is preferable to a Newtonian viscous model for analyzing the stresses involved in microboudinage of columnar tourmaline grains within the quartz matrix of the metamorphic tectonite. Tsubokawa and Ishikawa (2017) reported on the preparation of sub-micron polycrystalline olivine and clinopyroxene by sintering. Incorporation of trace amounts of graphite allows experimental investigations into the influence of graphite on mantle rheology and seismic velocity.

Authors' contributions

All authors of this article are guest editors for this special issue. All authors read and approved the final manuscript.

Author details

¹ Research Center for Earthquake Prediction, Disaster Prevention Research Institute, Kyoto University, Uji, Japan. ² Department of Geology, University of Otago, Dunedin 9054, New Zealand. ³ Department of Natural History Sciences, Graduate School of Sciences, Hokkaido University, Sapporo 060-0810, Japan. ⁴ Disaster Mitigation Research Center, Nagoya University, Furo-cho, Chikusa-ku, Nagoya 464-8601, Japan. ⁵ International Institute of Seismology

and Earthquake Engineering, Building Research Institute, Tsukuba, Japan. ⁶ Earth and Planetary Sciences, School of Science, Tokyo Institute of Technology, Tokyo, Japan.

Acknowledgements

We express our sincere gratitude to the authors who contributed to this special issue and the reviewers who evaluated the contributions and gave thoughtful comments and suggestions.

Competing interests

The authors declare that they have no competing interest.

Funding

This study was partly supported by the Ministry of Education, Culture, Sports, Science and Technology (MEXT) of Japan, under the Earthquake and Volcano Hazards Observation and Research Program, and KAKENHI Grant Numbers 26109001-26109007, and 15K21755.

Publisher's Note

Springer Nature remains neutral with regard to jurisdictional claims in published maps and institutional affiliations.

Received: 5 June 2018 Accepted: 6 June 2018

Published online: 20 June 2018

References

- Ando R, Imanishi K, Panayotopoulos Y, Kobayashi T (2017) Dynamic rupture propagation on geometrically complex fault with along-strike variation of fault maturity: insights from the 2014 Northern Nagano earthquake. *Earth Planets Space* 69:130. <https://doi.org/10.1186/s40623-017-0715-2>
- Dojo M, Hiramatsu Y (2017) Spatial variation in coda Q in the northeastern part of Niigata–Kobe Tectonic Zone, central Japan: implication of the cause of a high strain rate zone. *Earth Planets Space* 69:76. <https://doi.org/10.1186/s40623-017-0663-x>
- Fukuda J, Muto J, Nagahama H (2018) Strain localization and fabric development in polycrystalline anorthite + melt by water diffusion in an axial deformation experiment. *Earth Planets Space* 70:3. <https://doi.org/10.1186/s40623-017-0776-2>
- Hardebeck JL (2017) The spatial distribution of earthquake stress rotations following large subduction zone earthquakes. *Earth Planets Space* 69:69. <https://doi.org/10.1186/s40623-017-0654-y>
- lio Y, Yoneda I, Sawada M, Miura T, Katao H, Takada Y, Omura K, Horiuchi S (2017) Which is heterogeneous, stress or strength? An estimation from high-density seismic observations. *Earth Planets Space* 69:144. <https://doi.org/10.1186/s40623-017-0730-3>
- Kameda J, Inoue S, Tanikawa W, Yamaguchi A, Hamada Y, Hashimoto Y, Kimura G (2017) Alteration and dehydration of subducting oceanic crust within subduction zones: implications for décollement step-down and plate-boundary seismogenesis. *Earth Planets Space* 69:52. <https://doi.org/10.1186/s40623-017-0635-1>
- Kuwatani T, Toriumi M (2017) Thermodynamic forward modeling of retrogressive hydration reactions induced by geofluid infiltration. *Earth Planets Space* 69:18. <https://doi.org/10.1186/s40623-017-0607-5>
- Maeda S, Matsuzawa T, Toda S, Yoshida K, Katao H (2018) Complex microseismic activity and depth-dependent stress field changes in Wakayama, southwestern Japan. *Earth Planets Space* 70:21. <https://doi.org/10.1186/s40623-018-0788-6>
- Matsumoto N, Shigematsu N (2018) In-situ permeability of fault zones estimated by hydraulic tests and continuous groundwater-pressure observations. *Earth Planets Space* 70:13. <https://doi.org/10.1186/s40623-017-0765-5>
- Matsumura T, Kuwatani T, Masuda T (2017) Statistical model selection between elastic and Newtonian viscous matrix models for the microboudin palaeopiezometer. *Earth Planets Space* 69:83. <https://doi.org/10.1186/s40623-017-0669-4>
- Nakajima J, Matsuzawa T (2017) Anelastic properties beneath the Niigata–Kobe Tectonic Zone, Japan. *Earth Planets Space* 69:33. <https://doi.org/10.1186/s40623-017-0619-1>

- Nishimura T, Takada Y (2017) San-in shear zone in southwest Japan, revealed by GNSS observations. *Earth Planets Space* 69:85. <https://doi.org/10.1186/s40623-017-0673-8>
- Otsubo M, Miyakawa A, Imanishi K (2018) Normal-faulting stress state associated with low differential stress in an overriding plate in northeast Japan prior to the 2011 Mw 9.0 Tohoku earthquake. *Earth Planets Space* 70:51. <https://doi.org/10.1186/s40623-018-0813-9>
- Sibson RH (2017) Tensile overpressure compartments on low-angle thrust faults. *Earth Planets Space* 69:113. <https://doi.org/10.1186/s40623-017-0699-y>
- Sueoka S, Tagami T, Kohn BP (2017) First report of (U–Th)/He thermochronometric data across Northeast Japan Arc: implications for the long-term inelastic deformation. *Earth Planets Space* 69:79. <https://doi.org/10.1186/s40623-017-0661-z>
- Takada Y, Sagiya T, Nishimura T (2018) Interseismic crustal deformation in and around the Atotsugawa fault system, central Japan, detected by InSAR and GNSS. *Earth Planets Space* 70:32. <https://doi.org/10.1186/s40623-018-0801-0>
- Terakawa T (2017) Overpressurized fluids drive microseismic swarm activity around Mt. Ontake volcano, Japan. *Earth Planets Space* 69:87. <https://doi.org/10.1186/s40623-017-0671-x>
- Tsubokawa Y, Ishikawa M (2017) Sintering polycrystalline olivine and polycrystalline clinopyroxene containing trace amount of graphite from natural crystals. *Earth Planets Space* 69:128. <https://doi.org/10.1186/s40623-017-0717-0>
- Yukutake Y, Iio Y (2017) Why do aftershocks occur? Relationship between mainshock rupture and aftershock sequence based on highly resolved hypocenter and focal mechanism distributions. *Earth Planets Space* 69:68. <https://doi.org/10.1186/s40623-017-0650-2>
- Zhang X, Sagiya T (2017) Shear strain concentration mechanism in the lower crust below an intraplate strike-slip fault based on rheological laws of rocks. *Earth Planets Space* 69:82. <https://doi.org/10.1186/s40623-017-0668-5>

The spatial distribution of earthquake stress rotations following large subduction zone earthquakes

Jeanne L. Hardebeck

Earth, Planets and Space 2017, 69:69 DOI:10.1186/s40623-017-0654-y

Received: 27 January 2017, Accepted: 12 May 2017, Published: 18 May 2017

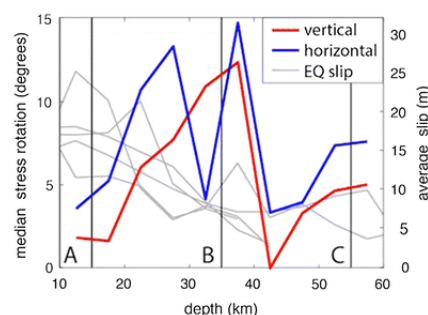
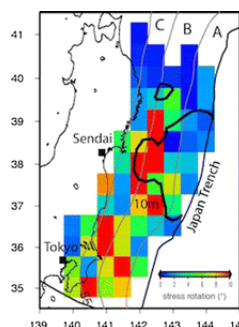


Abstract

Rotations of the principal stress axes due to great subduction zone earthquakes have been used to infer low differential stress and near-complete stress drop. The spatial distribution of coseismic and postseismic stress rotation as a function of depth and along-strike distance is explored for three recent $M \geq 8.8$ subduction megathrust earthquakes. In the down-dip direction, the largest coseismic stress rotations are found just above the Moho depth of the overriding plate. This zone has been identified as hosting large patches of large slip in great earthquakes, based on the lack of high-frequency radiated energy. The large continuous slip patches may facilitate near-complete stress drop. There is seismological evidence for high fluid pressures in the subducted slab around the Moho depth of the overriding plate, suggesting low differential stress levels in this zone due to high fluid pressure, also facilitating stress rotations. The coseismic stress rotations have similar along-strike extent as the

Postseismic stress rotations tend to occur in the same locations as the coseismic stress rotations, probably due to the very low remaining differential stress following the near-complete coseismic stress drop. The spatial complexity of the observed stress changes suggests that an analytical solution for finding the differential stress from the coseismic stress rotation may be overly simplistic, and that modeling of the full spatial distribution of the mainshock static stress changes is necessary.

Keywords: Stress, Subduction zone, Fault strength



Graphical abstract

Corresponding author: Jeanne L. Hardebeck, jhardebeck@usgs.gov

Thermodynamic forward modeling of retrogressive hydration reactions induced by geofluid infiltration

Tatsu Kuwatani* and Mitsuhiro Toriumi

Earth, Planets and Space 2017, 69:18 DOI:10.1186/s40623-017-0607-5

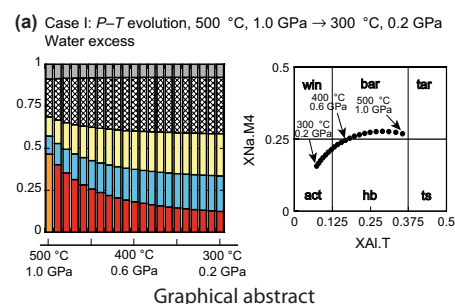
Received: 18 November 2016, Accepted: 20 January 2017, Published: 30 January 2017



Abstract

We have developed a new methodology for forward analysis of retrogressive hydration (rehydration) reactions by an improved thermodynamic forward modeling technique based on a differential thermodynamic approach (Gibbs' method). Based on natural observations and theoretical considerations, the progress of a rehydration reaction is modeled by incorporating a change in the effective bulk composition on account of the breakdown of the non-equilibrated phase and the amount of water infiltration into the system. Forward analyses of rehydration reactions under greenschist-facies conditions show that (1) the reaction progress of rehydration is proportional to the external water supply, and (2) the mineral compositions of equilibrated minerals are mainly controlled by P - T conditions and are similar to those in the global equilibrium model. Calculated results are in accordance with natural observations of rehydration reactions in greenschist-facies rocks, which supports the validity of the proposed model. The proposed model can be used as a basic forward model for various inversion analyses and numerical simulations and thus to understand the distribution and behavior of geofluids.

Keywords: Rehydration, Forward modeling, Greenschist, Geofluid



Graphical abstract

*Corresponding author: Tatsu Kuwatani, kuwatani@jamstec.go.jp

Alteration and dehydration of subducting oceanic crust within subduction zones: implications for décollement step-down and plate-boundary seismogenesis

Jun Kameda*, Sayako Inoue, Wataru Tanikawa, Asuka Yamaguchi, Yohei Hamada, Yoshitaka Hashimoto and Gaku Kimura

Earth, Planets and Space 2017, **69**:52 DOI:10.1186/s40623-017-0635-1

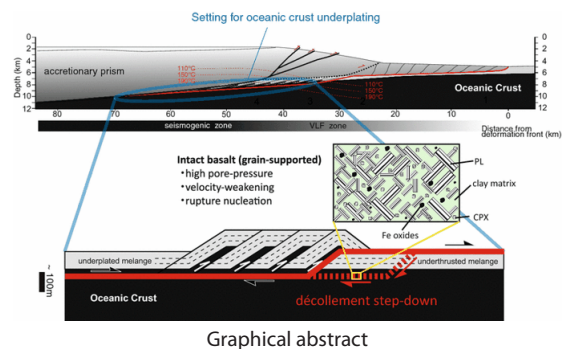
Received: 20 January 2017, Accepted: 6 April 2017, Published: 18 April 2017



Abstract

The alteration and dehydration of predominantly basaltic subducting oceanic crustal material are thought to be important controls on the mechanical and hydrological properties of the seismogenic plate interface below accretionary prisms. This study focuses on pillow basalts exposed in an ancient accretionary complex within the Shimanto Belt of southwest Japan and provides new quantitative data that provide insight into clay mineral reactions and the associated dehydration of underthrust basalts. Whole-rock and clay-fraction X-ray diffraction analyses indicate that the progressive conversion of saponite to chlorite proceeds under an almost constant bulk-rock mineral assemblage. These clay mineral reactions may persist to deep crustal levels (~320 °C), possibly contributing to the bulk dehydration of the basalt and supplying fluid to plate-boundary fault systems. This dehydration can also cause fluid pressurization at certain horizons within hydrous basalt sequences, eventually leading to fracturing and subsequent underplating of upper basement rock into the overriding accretionary prism. This dehydration-induced breakage of the basalt can explain variations in the thickness of accreted basalt fragments within accretionary prisms as well as the reported geochemical compositions of mineralized veins associated with exposed basalts in onland locations. This fracturing of intact basalt can also nucleate seismic rupturing that would subsequently propagate along seismogenic plate interfaces.

Keywords: Oceanic Crust, Vitritinite Reflectance, Accretionary Prism, Seismogenic Zone, Nankai Trough



*Corresponding author: Jun Kameda, kameda@sci.hokudai.ac.jp

Why do aftershocks occur? Relationship between mainshock rupture and aftershock sequence based on highly resolved hypocenter and focal mechanism distributions

Yohei Yukutake* and Yoshihisa Iio

Earth, Planets and Space 2017, **69**:68 DOI:10.1186/s40623-017-0650-2

Received: 9 January 2017, Accepted: 2 May 2017, Published: 15 May 2017



Abstract

In order to clarify the origin of aftershocks, we precisely analyze the hypocenters and focal mechanisms of the aftershocks following the 2000 Western Tottori Earthquake, which occurred in the western part of Japan, using data from dense seismic observations. We investigate whether aftershocks occur on the mainshock fault plane on which coseismic slip occurred or they represent the rupture of fractures surrounding the mainshock fault plane. Based on the hypocenter distribution of the aftershocks, the subsurface fault structure of the mainshock is estimated using principal component analysis. As a result, we can obtain the detail fault structure composed of 8 best-fit planes. We demonstrate that the aftershocks around the mainshock fault are distributed within zones of 1.0–1.5 km in thicknesses, and their focal mechanisms are significantly diverse. This result suggests that most of the aftershocks represent the rupture of fractures surrounding the mainshock fault rather than the rerupture of the mainshock fault. The aftershocks have a much wider zone compared with the exhumed fault zone in field observations, suggesting that many aftershocks occur outside the fault damage zone. We find that most aftershocks except in and around the large-slip region are well explained by coseismic stress changes. These results suggest that the thickness of the aftershock distribution may be controlled by the stress changes caused by the heterogeneous slip distribution during the mainshock. The aftershock is also distributed within a much wider zone than the hypocenter distribution observed in swarm activity in the geothermal region, which is thought to be caused by the migration of hydrothermal fluid. This result implies a difference in generation processes: Stress changes due to the mainshock contribute primarily to the occurrence of aftershocks, whereas earthquake swarms in the geothermal region are caused by fluid migration within the localized zone.

Keywords: Aftershock, Fault plane of mainshock, Fault damage zone, Hypocenter distribution, Focal mechanism

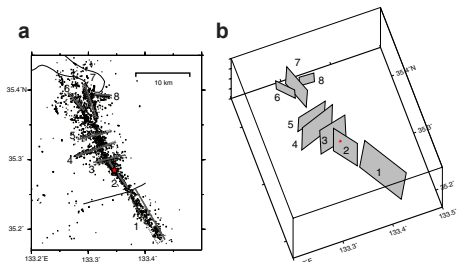


Fig. 4

*Corresponding author: Yohei Yukutake, yukutake@onken.odawara.kanagawa.jp

First report of (U–Th)/He thermochronometric data across Northeast Japan Arc: implications for the long-term inelastic deformation

Shigeru Sueoka*, Takahiro Tagami and Barry P. Kohn

Earth, Planets and Space 2017, **69**:79 DOI:10.1186/s40623-017-0661-z

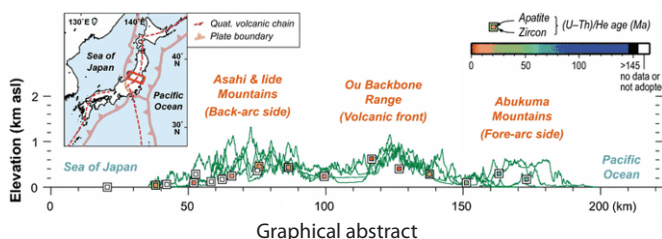
Received: 30 January 2017, Accepted: 29 May 2017, Published: 13 June 2017



Abstract

(U–Th)/He thermochronometric analyses were performed across the southern part of the Northeast Japan Arc for reconstructing the long-term uplift and denudation history in the region. Apatite (U–Th–Sm)/He ages ranged from 64.3 to 1.5 Ma, while zircon (U–Th)/He ages ranged between 39.6 and 11.0 Ma. Apatite (U–Th–Sm)/He ages showed obvious contrast among the morphostructural provinces; older ages of 64.3–49.6 Ma were obtained in the Abukuma Mountains on the fore-arc side, whereas younger ages of 11.4–1.5 Ma were determined in the Ou Backbone Range (OBR) along the volcanic front and the Asahi Mountains on the back-arc side. The age contrasts are basically interpreted to reflect the differences in the uplift and the denudation histories of the provinces considering the thermal effects of magmatism and timing of the known uplift episodes. Denudation rates were calculated to be <math><0.1</math> mm/year in the Abukuma Mountains, ~0.1 to 1 mm/year in the Ou Backbone Range, and ~0.1 to 0.3 mm/year in the Asahi Mountains. The denudation rates tend to increase from the mountain base to the ridges in the OBR (and the Asahi Mountains). This relationship shows a contrast with the previous findings in fault-block mountains in the Southwest (SW) Japan Arc, where the highest denudation rates were estimated near fault(s) along the base(s). This observation might reflect a difference in mountain uplift mechanisms between the NE and the SW Japan Arcs and imply that thermochronometric approaches are useful for constraining uplift and denudation histories at the scale of an island arc, as well as continental orogens. However, careful discussion of magmatic thermal effects is required.

Keywords: (U–Th)/He thermochronometry, Denudation, Inelastic deformation, Northeast Japan Arc



*Corresponding author: Shigeru Sueoka, sueoka.shigeru@jaea.go.jp

Shear strain concentration mechanism in the lower crust below an intraplate strike-slip fault based on rheological laws of rocks

Xuelei Zhang* and Takeshi Sagiya

Earth, Planets and Space 2017, **69**:82 DOI:10.1186/s40623-017-0668-5

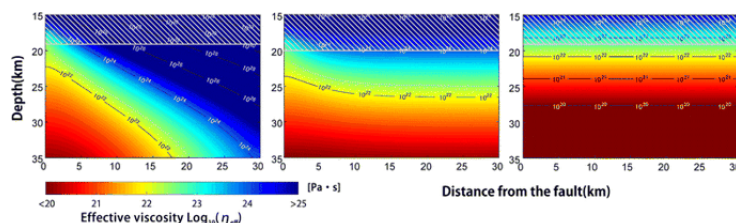
Received: 5 February 2017, Accepted: 8 June 2017, Published: 19 June 2017



Abstract

We conduct a two-dimensional numerical experiment on the lower crust under an intraplate strike-slip fault based on laboratory-derived power-law rheologies considering the effects of grain size and water. To understand the effects of far-field loading and material properties on the deformation of the lower crust on a geological time scale, we assume steady fault sliding on the fault in the upper crust and ductile flow for the lower crust. To avoid the stress singularity, we introduce a yield threshold in the brittle–ductile transition near the down-dip edge of the fault. Regarding the physical mechanisms for shear strain concentration in the lower crust, we consider frictional and shear heating, grain size, and power-law creep. We evaluate the significance of these mechanisms in the formation of the shear zone under an intraplate strike-slip fault with slow deformation. The results show that in the lower crust, plastic deformation is possible only when the stress or temperature is sufficiently high. At a similar stress level, ~100 MPa, dry anorthite begins to undergo plastic deformation at a depth around 28–29 km, which is about 8 km deeper than wet anorthite. As a result of dynamic recrystallization and grain growth, the grain size in the lower crust may vary laterally and as a function of depth. A comparison of the results with constant and non-constant grain sizes reveals that the shear zone in the lower crust is created by power-law creep and is maintained by dynamically recrystallized material in the shear zone because grain growth occurs in a timescale much longer than the recurrence interval of intraplate earthquakes. Owing to the slow slip rate, shear and frictional heating have negligible effects on the deformation of the shear zone. The heat production rate depends weakly on the rock rheology; the maximum temperature increase over 3 Myr is only about several tens of degrees.

Keywords: Intraplate strike-slip fault, 2-D thermal-mechanical fault model, Ductile shear zone



Graphical abstract

*Corresponding author: Xuelei Zhang, zhang@seis.nagoya-u.ac.jp

Statistical model selection between elastic and Newtonian viscous matrix models for the microboudin palaeopiezometer

Tarojiro Matsumura*, Tatsu Kuwatani and Toshiaki Masuda

Earth, Planets and Space 2017, **69**:83 DOI:10.1186/s40623-017-0669-4

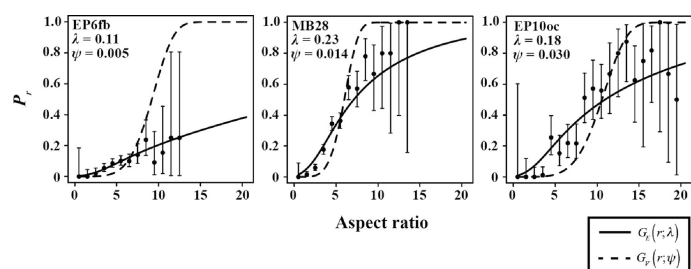
Received: 27 January 2017, Accepted: 8 June 2017, Published: 22 June 2017



Abstract

We carried out statistical evaluations of two probability density functions for the microboudin palaeopiezometer using the Akaike information criterion (AIC) and the cross-validation (CV) technique. In terms of the relevant stress-transfer model, these functions are defined as the elastic matrix model and the Newtonian viscous matrix model, respectively. The AIC and CV techniques enable us to evaluate the relative quality of both models when applied to nine data sets collected from metachert samples containing tourmaline grains in a quartz matrix, collected from the East Pilbara Terrane, Western Australia. The results show that the elastic matrix model is the more appropriate probability density function for analysis of fracturing of tourmaline grains in a quartz matrix. This statistical evaluation shows the validity of the elastic matrix model for the microboudin palaeopiezometer when analysing such data sets.

Keywords: Microboudinage structure, AIC, Cross-validation, Statistical model selection, Elastic matrix model, Newtonian viscous matrix model



*Corresponding author: Tarojiro Matsumura, matsumura-tarojiro@aist.go.jp; f5344007@ipc.shizuoka.ac.jp

Overpressurized fluids drive microseismic swarm activity around Mt. Ontake volcano, Japan

Toshiko Terakawa

Earth, Planets and Space 2017, **69**:87 DOI:10.1186/s40623-017-0671-x

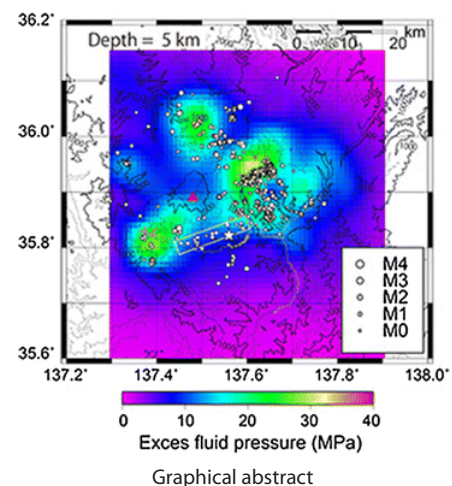
Received: 24 March 2017, Accepted: 20 June 2017, Published: 29 June 2017



Abstract

Microseismic swarm activity has taken place since 1976 around Mt. Ontake, the second highest stratovolcano in Japan. This activity is thought to be linked to high pore-fluid pressure in the vicinity of the volcano. We analyzed well-constrained focal mechanism solutions of microseismicity to re-estimate the 3-D pore-fluid pressure field driving vigorous swarm activity around Mt. Ontake. Pore-fluid pressures were measured by mapping earthquake focal mechanisms on the 3-D Mohr diagram for the regional stress field with high resolutions of 2–5 km. The assumption of the reference stress pattern can cause modeling errors in measurements of pore-fluid pressure. To remove the effect, we statistically evaluated the estimation errors of the regional stress field and included these errors in the analysis. We detected an overpressurized fluid reservoir with a peak of about 10–30 MPa in the east flank of Mt. Ontake, where microseismic swarm activity has been vigorous for the last two decades. The level of pore-fluid pressure was maintained for at least 5 years after 2009. This finding indicates that there are some interactions between the intensive swarm activity and overpressurized fluids: the swarm activity has been driven by overpressurized fluids, whereas pore-fluid pressures have been suppressed by the swarm activity.

Keywords: Pore-fluid pressures, Seismic swarm, Stress field, Earthquake focal mechanisms, Inversion theory



Corresponding author: Toshiko Terakawa, terakawa@seis.nagoya-u.ac.jp

Tensile overpressure compartments on low-angle thrust faults

Richard H. Sibson

Earth, Planets and Space 2017, 69:113 DOI:10.1186/s40623-017-0699-y

Received: 8 April 2017, Accepted: 31 July 2017, Published: 15 August 2017



Abstract

Hydrothermal extension veins form by hydraulic fracturing under triaxial stress (principal compressive stresses, $\sigma_1 > \sigma_2 > \sigma_3$) when the pore-fluid pressure, P_f , exceeds the least compressive stress by the rock's tensile strength. Such veins form perpendicular to σ_3 , their incremental precipitation from hydrothermal fluid often reflected in 'crack-seal' textures, demonstrating that the tensile overpressure state, $\sigma_3' = (\sigma_3 - P_f) < 0$, was repeatedly met. Systematic arrays of extension veins develop locally in both sub-metamorphic and metamorphic assemblages defining *tensile overpressure compartments* where at some time $P_f > \sigma_3$. In compressional regimes ($\sigma_v = \sigma_3$), subhorizontal extension veins may develop over vertical intervals < 1 km or so below low-permeability sealing horizons with tensile strengths $10 < T_o < 20$ MPa. This is borne out by natural vein arrays. For a low-angle thrust, the vertical interval where the tensile overpressure state obtains may continue down-dip over distances of several kilometres in some instances.

The overpressure condition for hydraulic fracturing is comparable to that needed for frictional reshear of a thrust fault lying close to the maximum compression, σ_1 . Under these circumstances, especially where the shear zone material has varying competence (tensile strength), affecting the failure mode, dilatant fault–fracture mesh structures may develop throughout a tabular rock volume. Evidence for the existence of fault–fracture meshes around low-angle thrusts comes from exhumed ancient structures and from active structures. In the case of megathrust ruptures along subduction interfaces, force balance analyses, lack of evidence for shear heating, and evidence of total shear stress release during earthquakes suggest the interfaces are extremely weak ($\tau < 40$ MPa), consistent with weakening by near-lithostatically overpressured fluids. Portions of the subduction interface, especially towards the down-dip termination of the seismogenic megathrust, are prone to episodes of slow-slip, non-volcanic tremor, low-frequency earthquakes, very-low-frequency earthquakes, etc., attributable to the activation of tabular fault–fracture meshes at low σ_3' around the thrust interface. Containment of near-lithostatic overpressures in such settings is precarious, fluid loss curtailing mesh activity.

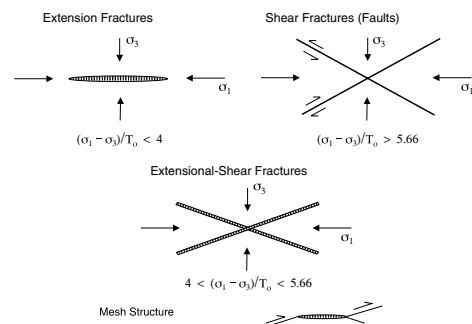


Fig. 1

Corresponding author: Richard H. Sibson, rick.sibson@otago.ac.nz

Dynamic rupture propagation on geometrically complex fault with along-strike variation of fault maturity: insights from the 2014 Northern Nagano earthquake

Ryosuke Ando*, Kazutoshi Imanishi, Yannis Panayotopoulos and Tomokazu Kobayashi

Earth, Planets and Space 2017, 69:130 DOI:10.1186/s40623-017-0715-2

Received: 4 April 2017, Accepted: 5 September 2017, Published: 18 September 2017

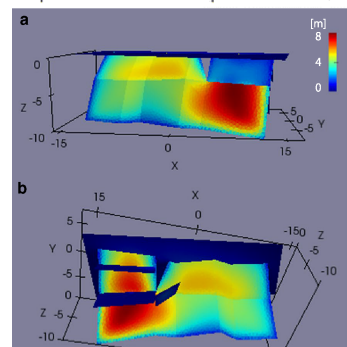


Abstract

Understanding the effect of the complex fault geometry on the dynamic rupture process and discriminating it from the complexity originating from the rheological properties of faults, is an essential subject in earthquake science. The 2014 Northern Nagano earthquake, which occurred near the end zone of a major active fault system, provided unique observations that enabled us to investigate both the detailed geometrical fault structure and surface deformation patterns as well as the temporal sequence led up from a prominent foreshock activity. We first develop a geometrical fault model with a substantial variation along strike, and a model for the regional stress field, which is well constrained by the observations. This significant along-strike variation in fault geometry probably reflects the difference of fault maturity at the end zone of the complex fault system. We used this model in order to conduct a set of dynamic rupture simulations using the highly efficient spatiotemporal boundary integral equation method. Based on our simulations, we show that the observed surface deformation can be reasonably explained as the effect of the non-planar fault geometry with a number of branch faults and bends.

Keywords: 2014 Northern Nagano earthquake, Fault geometry, Dynamic rupture, InSAR, Fast domain partitioning BIEM

Slip distributions on 3-D non-planar fault surfaces



Graphical abstract

*Corresponding author: Ryosuke Ando, ando@eps.s.u-tokyo.ac.jp

Which is heterogeneous, stress or strength? An estimation from high-density seismic observations

Yoshihisa Iio*, Itaru Yoneda, Masayo Sawada, Tsutomu Miura, Hiroshi Katao, Yoichiro Takada, Kentaro Omura and Shigeki Horiuchi

Earth, Planets and Space 2017, 69:144 DOI:10.1186/s40623-017-0730-3

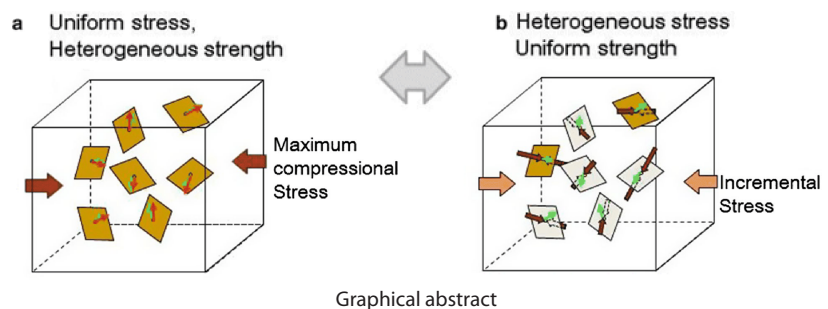
Received: 22 April 2017, Accepted: 11 October 2017, Published: 20 October 2017



Abstract

Using data from high-density seismic observation networks installed in the western Nagano Prefecture region in Japan, we precisely determined focal mechanisms and estimated the high-resolution stress field at a scale of 1 km. Almost all differences between observed and calculated slip directions (misfit) were smaller than the errors in focal mechanisms at grid points away from the mainshock fault. This finding clearly indicates that the estimated uniform stress suitably explains focal mechanisms in each subregion apart from the mainshock fault. Misfits are relatively large at grid points near the mainshock fault, but many of these misfits are smaller than the errors in focal mechanisms, and stress is regarded as uniform for a greater portion within each subregion. However, we found that focal mechanisms and *P*-axes varied widely and differed from each other for a short focal distance of 100 m. These results clearly show that stress can be regarded as uniform, but that strength is heterogeneous.

Keywords: Stress, Heterogeneity, Fault strength, Stress inversion, Focal mechanism



*Corresponding author: Yoshihisa Iio, iio@rcep.dpri.kyoto-u.ac.jp

Strain localization and fabric development in polycrystalline anorthite + melt by water diffusion in an axial deformation experiment

Jun-ichi Fukuda*, Jun Muto and Hiroyuki Nagahama

Earth, Planets and Space 2018, 70:3 DOI:10.1186/s40623-017-0776-2

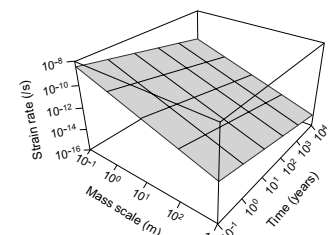
Received: 31 March 2017, Accepted: 26 December 2017, Published: 4 January 2018



Abstract

We performed two axial deformation experiments on synthetic polycrystalline anorthite samples with a grain size of $\sim 3 \mu\text{m}$ and 5 vol% Si–Al-rich glass at 900 °C, a confining pressure of 1.0 GPa, and a strain rate of $10^{-4.8} \text{ s}^{-1}$. One sample was deformed as-is (dry); in the other sample, two half-cut samples (two cores) with 0.15 wt% water at the boundary were put together in the apparatus. The mechanical data for both samples were essentially identical with a yield strength of $\sim 700 \text{ MPa}$ and strain weakening of $\sim 500 \text{ MPa}$ by 20% strain. The dry sample appears to have been deformed by distributed fracturing. Meanwhile, the water-added sample shows plastic strain localization in addition to fracturing and reaction products composed of zoisite grains and SiO_2 materials along the boundary between the two sample cores. Infrared spectra of the water-added sample showed dominant water bands of zoisite. The maximum water content was 1500 wt ppm H_2O at the two-core boundary, which is the same as the added amount. The water contents gradually decreased from the boundaries to the sample interior, and the gradient fitted well with the solution of the one-dimensional diffusion equation. The determined diffusion coefficient was $7.4 \times 10^{-13} \text{ m}^2/\text{s}$, which agrees with previous data for the grain boundary diffusion of water. The anorthite grains in the water-added sample showed no crystallographic preferred orientation. Textural observations and water diffusion indicate that water promotes the plastic deformation of polycrystalline anorthite by grain-size-sensitive creep as well as simultaneous reactions. We calculated the strain rate evolution controlled by water diffusion in feldspar aggregates surrounded by a water source. We assumed water diffusion in a dry rock mass with variable sizes. Diffused water weakens a rock mass with time under compressive stress. The calculated strain rate decreased from 10^{-10} to 10^{-15} s^{-1} with an increase in the rock mass size to which water is supplied from $< 1 \text{ m}$ to 1 km and an increase in the time of water diffusion from < 1 to $\sim 10,000$ years. This indicates a decrease in the strain rate in a rock mass with increasing deformation via water diffusion.

Keywords: Anhydrous polycrystalline anorthite, Water diffusion, Griggs-type deformation apparatus, Plastic deformation, Reaction



*Corresponding author: Jun-ichi Fukuda, jfukuda@eps.s.u-tokyo.ac.jp

In-situ permeability of fault zones estimated by hydraulic tests and continuous groundwater-pressure observations

Norio Matsumoto* and Norio Shigematsu

Earth, Planets and Space 2018, **70**:13 DOI:10.1186/s40623-017-0765-5

Received: 31 March 2017, Accepted: 19 December 2017, Published: 25 January 2018



Abstract

In-situ permeability of the Median Tectonic Line (MTL) fault zone in Mie Prefecture, southwest Japan, was estimated using hydraulic tests and groundwater pressure observations in two boreholes. The screen depths in Holes 1 and 2 are located, respectively, in a major strand of the MTL fault zone within the Sambagawa metamorphic rocks and a branching fault developed in the hanging wall of the MTL within the Ryoke mylonite. The estimated permeability at Hole 1 ranges from 5.3×10^{-17} to 5.0×10^{-16} m², and that at Hole 2 ranges from 4.4×10^{-16} to 1.5×10^{-15} m². We also measured the permeability of the protolith close to the screened depth of Hole 1 (3.4×10^{-19} and 3.7×10^{-19} m²) and Hole 2 (3.1×10^{-19} and 6.2×10^{-19} m²). The permeability of the fault zone was found to be more than 100 and 700 times higher than the protolith permeability at Holes 1 and 2, respectively. The permeability data for Holes 1 and 2 are consistent with previously reported permeability data for samples from an MTL outcrop. The permeability observed in this study reflects the complex fault zone permeability structure of the MTL fault zone.

Keywords: Fault zone permeability, Slug test, Pumping test, Permeability of drillcore sample, Median Tectonic Line

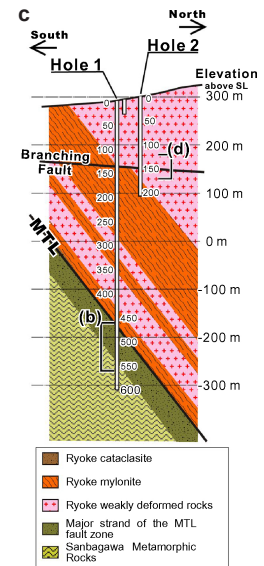


Fig. 1

*Corresponding author: Norio Matsumoto, n.matsumoto@aist.go.jp

Complex microseismic activity and depth-dependent stress field changes in Wakayama, southwestern Japan

Sumire Maeda*, Toru Matsuzawa, Shinji Toda, Keisuke Yoshida and Hiroshi Katao

Earth, Planets and Space 2018, **70**:21 DOI:10.1186/s40623-018-0788-6

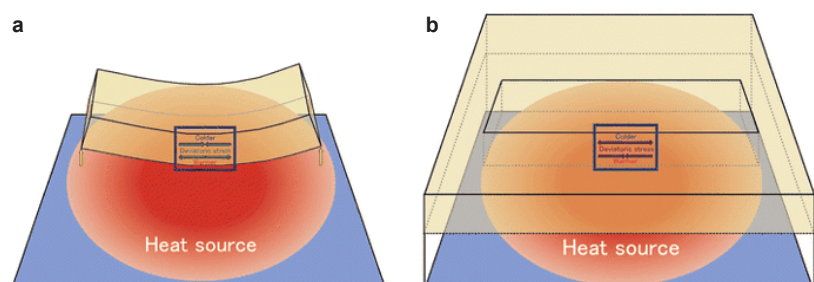
Received: 25 March 2017, Accepted: 24 January 2018, Published: 7 February 2018



Abstract

We examined the spatial relationship between seismicity and upper crustal structure in the Wakayama region, northwestern Kii Peninsula, Japan, by investigating microearthquake focal mechanisms and the local stress field. The focal mechanisms of most events studied fall into three categories: (1) normal faulting with N–S-oriented T-axes mainly occurring at shallow depths, (2) reverse faulting with E–W-oriented P-axes dominating at intermediate depths, and (3) strike-slip faulting with N–S-oriented T-axes and E–W-oriented P-axes mainly seen at greater depths. The stress field varies with depth: the shallow part is characterized by a strike-slip-type stress regime with N–S tension and E–W compression, while the deep part is characterized by an E–W compressional stress regime consistent with reverse faulting. The depth-dependent stress regime can be explained by thermal stress caused by a heat source, as expected from geophysical observations. Geologic faults, acting as weak planes, might contribute to generate shallow normal fault-type and deeper strike-slip fault-type microearthquakes.

Keywords: Microearthquake, Stress field, Heterogeneous structure, Fluid, Heat source, Geological structure



Graphical abstract

*Corresponding author: Sumire Maeda, maeda.sumire.q6@dc.tohoku.ac.jp

Interseismic crustal deformation in and around the Atotsugawa fault system, central Japan, detected by InSAR and GNSS

Youichiro Takada*, Takeshi Sagiya and Takuya Nishimura

Earth, Planets and Space 2018, **70**:32 DOI:10.1186/s40623-018-0801-0

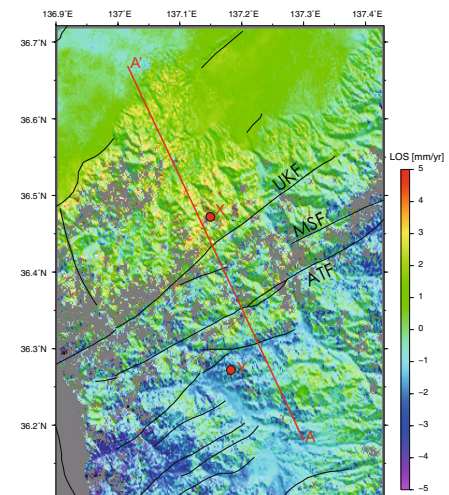
Received: 31 March 2017, Accepted: 7 February 2018, Published: 16 February 2018



Abstract

The Atotsugawa fault system is one of the best-known active faults in Japan. However, revealing the interseismic velocity field in and around the Atotsugawa fault system with high spatial resolution is challenging because of dense vegetation, steep topography, and heavy snowfall in winter. To overcome these difficulties, we combined ALOS/PALSAR data and GNSS data from our original stations in addition to the nationwide station network (GEONET). First, we removed the height-dependent phase change in each interferogram using a digital elevation model. Next, we removed the long-wavelength phase trend using the GNSS velocity field. Finally, we applied an InSAR time-series analysis, known as small baseline subset analysis (SBAS), to all the corrected interferograms. The resultant mean velocity field shows a remarkable phase gradient around the Atotsugawa fault system. We found a sharp velocity gradient across the Ushikubi fault, a major strand of the Atotsugawa faults system, rather than the main trace of the Atotsugawa fault. Using InSAR, we found that the interseismic deformation inside the strain concentration zone is spatially heterogeneous and different from what we expect from the fault traces.

Keywords: InSAR, GNSS, Atotsugawa fault, Interseismic velocity



Graphical abstract

*Corresponding author: Youichiro Takada, takaday@sci.hokudai.ac.jp

Normal-faulting stress state associated with low differential stress in an overriding plate in northeast Japan prior to the 2011 Mw 9.0 Tohoku earthquake

Makoto Otsubo*, Ayumu Miyakawa and Kazutoshi Imanishi

Earth, Planets and Space 2018, **70**:51 DOI:10.1186/s40623-018-0813-9

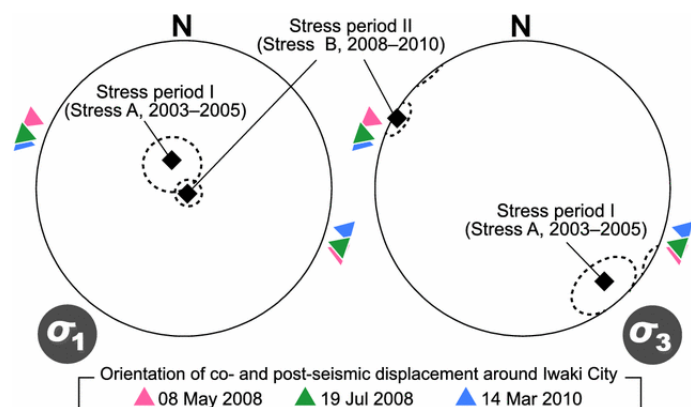
Received: 27 January 2017, Accepted: 7 March 2018, Published: 26 March 2018



Abstract

Spatial and temporal variations in inland crustal stress prior to the 2011 Mw 9.0 Tohoku earthquake are investigated using focal mechanism solutions for shallow seismicity in Iwaki City, Japan. The multiple inverse method of stress tensor inversion detected two normal-faulting stress states that dominate in different regions. The stress field around Iwaki City changed from a NNW–SSE-trending triaxial extensional stress (stress regime A) to a NW–SE-trending axial tension (stress regime B) between 2005 and 2008. These stress changes may be the result of accumulated extensional stress associated with co- and post-seismic deformation due to the M7 class earthquakes. In this study we suggest that the stress state around Iwaki City prior to the 2011 Tohoku earthquake may have been extensional with a low differential stress. High pore pressure is required to cause earthquakes under such small differential stresses.

Keywords: Crustal stress, 2011 Tohoku earthquake, Deformation, Stress tensor inversion, Differential stress



Graphical abstract

*Corresponding author: Makoto Otsubo, otsubo-m@aist.go.jp

Anelastic properties beneath the Niigata–Kobe Tectonic Zone, Japan

Junichi Nakajima* and Toru Matsuzawa

Earth, Planets and Space 2017, **69**:33 DOI:10.1186/s40623-017-0619-1

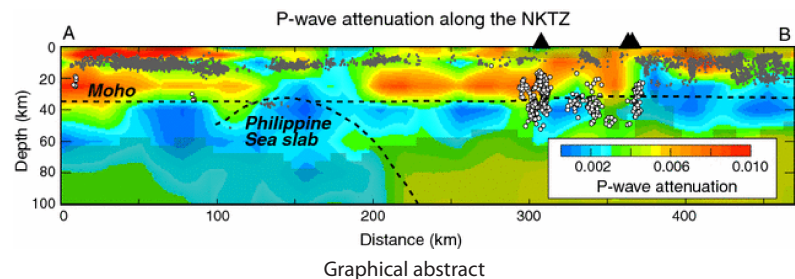
Received: 11 January 2017, Accepted: 13 February 2017, Published: 22 February 2017



Abstract

We estimate the three-dimensional (3D) P-wave attenuation structure beneath the Niigata–Kobe Tectonic Zone (NKTZ), central Japan, using high-quality waveform data from a large number of stations. The obtained results confirm the segmentation of the NKTZ into three regions, as suggested by 3D seismic velocity models, and reveal characteristic structures related to surface deformation, shallow subduction of the Philippine Sea slab, and magmatism. The lower crust beneath the NKTZ west of the Itoigawa–Shizuoka Tectonic Line (ISTL) is overall characterized by distinct high attenuation, whereas the upper crust shows marked high attenuation to the east of the ISTL. Differences in the depths of anelastically weakened parts of the crust probably result in a first-order spatial variation in surface deformation, forming wide (width of ~100 km) and narrow (width of 25–40 km) deformation zones on the western and eastern sides of the ISTL, respectively. Many $M \geq 6.5$ earthquakes occur in the upper crust where seismic attenuation in the underlying lower crust varies sharply, suggesting that spatial variations in rates of anelastic deformation in the lower crust result in stress concentration in the overlying brittle crust. We interpret a moderate- to low-attenuation zone located in the lower crust at the northeast of Biwa Lake to reflect low-temperature conditions that are developed locally as a result of shallow subduction of the cold Philippine Sea slab.

Keywords: Seismic attenuation, Strain, Surface deformation, Slab, Grain size



*Corresponding author: Junichi Nakajima, nakajima@geo.titech.ac.jp

Spatial variation in coda Q in the northeastern part of Niigata–Kobe Tectonic Zone, central Japan: implication of the cause of a high strain rate zone

Masanobu Dojo and Yoshihiro Hiramatsu*

Earth, Planets and Space 2017, **69**:76 DOI:10.1186/s40623-017-0663-x

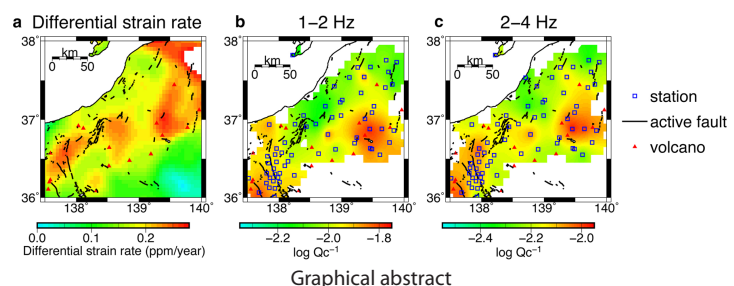
Received: 26 January 2017, Accepted: 29 May 2017, Published: 5 June 2017



Abstract

We have analyzed the spatial variation in coda Q in the northeastern part of a high strain rate zone, the Niigata–Kobe Tectonic Zone (NKTZ), to investigate the cause of the high strain rate by correlating coda Q with the differential strain rate and the S-wave velocity. The spatial distributions of coda Q in the 2–4 and 4–8 Hz frequency bands are found to be negatively correlated with the differential strain rate. Coda Q in the 2–4 Hz frequency band is correlated spatially with the S-wave velocity at a 25 km depth, as has been reported previously. We also find a positive correlation between the perturbation of the S-wave velocity at a 10 km depth and coda Q in the 4–8 Hz frequency band, implying that the spatial distribution of coda Q in this frequency band is mainly attributed to the heterogeneity of the upper crust. This feature is different from that of the central part of the NKTZ reported previously, which indicates a difference in the cause of the high strain rate. Therefore, we suggest that the high deformation rate in the upper crust, which is characterized by a thick sediment basin, as well as that in the ductile lower crust, contributes to the generation process of the high strain rate on the surface in the northeastern part of the NKTZ.

Keywords: Heterogeneity, Differential strain rate, S-wave velocity, Ductile deformation



*Corresponding author: Yoshihiro Hiramatsu, yoshizo@staff.kanazawa-u.ac.jp

San-in shear zone in southwest Japan, revealed by GNSS observations

Takuya Nishimura* and Youichiro Takada

Earth, Planets and Space 2017, **69**:85 DOI:10.1186/s40623-017-0673-8

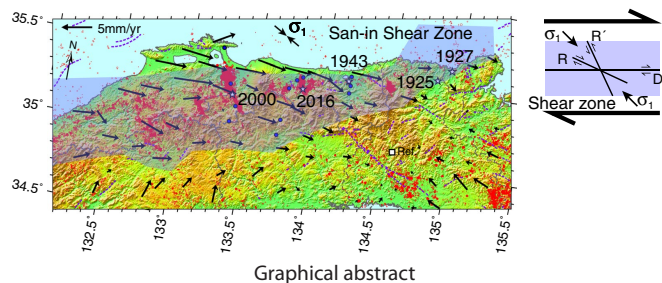
Received: 30 March 2017, Accepted: 20 June 2017, Published: 27 June 2017



Abstract

A right-lateral shear zone in the San-in region, southwest Japan, has been proposed by previous geological and seismological studies. It locates 350 km north of the Nankai Trough, that is, the main plate boundary between the subducting Philippine Sea and overriding Amurian plates and presumably accommodates a part of the relative plate motion. We present a geodetic evidence of the proposed shear zone using GNSS velocity data. Distinct shear deformation is identified only between $\sim 132.5^\circ\text{E}$ and $\sim 135^\circ\text{E}$ along a coastline which is a part of the proposed shear zone, and we propose to call the geodetically identified shear zone as the San-in shear zone (SSZ). The SSZ is a concentrated deformation zone with a width of ~ 50 km and can be modeled by a deep creep on a vertical strike slip fault with a creep rate of ~ 5 mm/year. There are some active faults parallel and oblique to the overall trend of the SSZ, but no single active fault coincides with the SSZ. Lineaments of microseismicity and source faults of large earthquakes are almost oriented in NNW–SSE in the SSZ and oblique to the overall trend of the SSZ. They are interpreted as conjugate Riedel shears. Based on these geodetic, seismological, and geomorphological observations, we suggest that the SSZ is a developing and young shear zone in a geological time scale.

Keywords: San-in shear zone (SSZ), Strain concentration zone, GNSS, Southwest Japan



*Corresponding author: Takuya Nishimura, nishimura.takuya.4s@kyoto-u.ac.jp

Sintering polycrystalline olivine and polycrystalline clinopyroxene containing trace amount of graphite from natural crystals

Yumiko Tsubokawa* and Masahiro Ishikawa

Earth, Planets and Space 2017, **69**:128 DOI:10.1186/s40623-017-0717-0

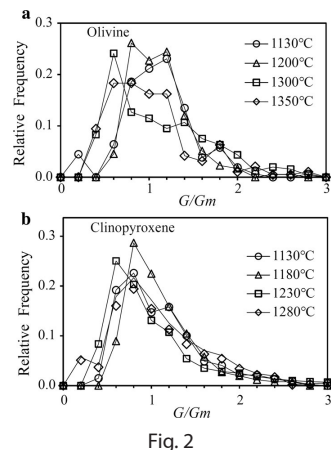
Received: 9 April 2017, Accepted: 7 September 2017, Published: 16 September 2017



Abstract

Graphite-bearing polycrystalline olivine and polycrystalline clinopyroxene with submicron to micron grain size were successfully sintered from a single crystal of naturally occurring olivine ($\text{Fo}_{88-92}\text{Fa}_{12-8}\text{Mg}_{1.76-1.84}\text{Fe}_{0.16-0.24}\text{SiO}_4$) and a single crystal of naturally occurring clinopyroxene ($\text{Di}_{99}\text{Hed}_1\text{Ca}_{0.92}\text{Na}_{0.07}\text{Mn}_{0.01}\text{Mg}_{0.93}\text{Fe}_{0.01}\text{Al}_{0.06}\text{Si}_2\text{O}_6$). The milled powders of both these crystals were sintered under argon gas flow at temperatures ranging from 1130 to 1350 °C for 2 h. As the sintering temperature increased, the average grain size of olivine increased from 0.2 to 1.4 μm and that of clinopyroxene increased from 0.1 to 2.4 μm . The porosity of sintered samples remained at an almost-constant volume of 2–5% for olivine and 3–4% for clinopyroxene. The samples sintered from powders milled with ethanol exhibited trace amount of graphite, identified via Raman spectroscopy analysis. As the sintering temperature increased, the intensity of the graphite Raman peak decreased, compared with both olivine and clinopyroxene peaks. The carbon content of the sintered samples was estimated to be a few hundred ppm. The in-plane size (L_p) of graphite in the sintered olivine was estimated to be < 15 nm. Our experiments demonstrate new possibilities for preparing graphite-bearing silicate-mantle mineral rocks, and this method might be useful in understanding the influence of the physical properties of graphite on grain-size-sensitive rheology or the seismic velocity of the Earth's mantle.

Keywords: Graphite, Olivine, Clinopyroxene, Submicron



*Corresponding author: Yumiko Tsubokawa, tsubokawa-yumiko-nd@ynu.jp

Information for Contributors

General

1. Manuscripts should be submitted through the journal's Editorial Manager system (<https://www.editorialmanager.com/epsp/default.aspx>).
2. Only papers not previously published will be accepted, and the emphasis is on the originality of concept or observation.
3. Four varieties of article types are available.
 - 3.1 "Full Papers" without word limit.
 - 3.2 "Express Letters" have a limit of 5000 words including the title page, abstract, keywords, main text, declarations, references, figure legends and table legends. The sum of the number of figures and tables should be less than or equal to 5.
 - 3.3 "Frontier Letters" can be submitted upon invitation by the Editor-in-Chief.
 - 3.4 "Technical Reports" describe the technical development of instrument or software.
 - 3.5 "Comment" is a substantial re-analysis of a previously published article in the journal. "Comment" should not exceed 1000 words.
4. Authors retain the copyright, and distribution of articles is free under the CC BY license.

Technical

1. Manuscripts should be written in English with double spacing.
2. Each manuscript should be organized in the following order: title, authors' names, affiliations, abstract, key words, main text, acknowledgement, appendix, references, and supplementary materials. A graphical abstract image must be uploaded during submission which should provide the reader with a visual description of the topic covered in the article.
3. The corresponding author should be clearly indicated.
4. The abstract is limited to 300 words and should be informative and include principal findings and conclusions. Please avoid abbreviations.
5. The main text can have multiple free headings.
6. High-resolution figures should be provided in the following format; PDF (preferred format for diagrams), PNG (preferred format for photos or images), EPS, TIFF, JPEG, BMP. The graphical abstract should be approximately 920 × 300 pixels and should be uploaded as a JPEG, PNG or SVG file.
7. References must follow the Springer Basic style.

Correspondence

If you have any questions, please contact editorial@earth-planets-space.com.

© EPS Steering Committee 2019 All rights reserved.

A Grant-in-Aid for Publication of Scientific Research Results (19HP1001) from Japan Society for the Promotion of Science is used for printing.

Contents

Crustal dynamics: unified understanding of geodynamic processes at different time and length scales Yoshihisa Iio, Richard H. Sibson, Toru Takeshita, Takeshi Sagiya, Bunichiro Shibazaki and Junichi Nakajima	1
The spatial distribution of earthquake stress rotations following large subduction zone earthquakes Jeanne L. Hardebeck	5
Thermodynamic forward modeling of retrogressive hydration reactions induced by geofluid infiltration Tatsu Kuwatani and Mitsuhiro Toriumi	5
Alteration and dehydration of subducting oceanic crust within subduction zones: implications for décollement step-down and plate-boundary seismogenesis..... Jun Kameda, Sayako Inoue, Wataru Tanikawa, Asuka Yamaguchi, Yohei Hamada, Yoshitaka Hashimoto and Gaku Kimura	6
Why do aftershocks occur? Relationship between mainshock rupture and aftershock sequence based on highly resolved hypocenter and focal mechanism distributions..... Yohei Yukutake and Yoshihisa Iio	6
First report of (U–Th)/He thermochronometric data across Northeast Japan Arc: implications for the long-term inelastic deformation..... Shigeru Sueoka, Takahiro Tagami and Barry P. Kohn	7
Shear strain concentration mechanism in the lower crust below an intraplate strike-slip fault based on rheological laws of rocks..... Xuelei Zhang and Takeshi Sagiya	7
Statistical model selection between elastic and Newtonian viscous matrix models for the microboudin palaeopiezometer..... Tarojiro Matsumura, Tatsu Kuwatani and Toshiaki Masuda	8
Overpressurized fluids drive microseismic swarm activity around Mt. Ontake volcano, Japan..... Toshiko Terakawa	8
Tensile overpressure compartments on low-angle thrust faults..... Richard H. Sibson	9
Dynamic rupture propagation on geometrically complex fault with along-strike variation of fault maturity: insights from the 2014 Northern Nagano earthquake Ryosuke Ando, Kazutoshi Imanishi, Yannis Panayotopoulos and Tomokazu Kobayashi	9
Which is heterogeneous, stress or strength? An estimation from high-density seismic observations Yoshihisa Iio, Itaru Yoneda, Masayo Sawada, Tsutomu Miura, Hiroshi Katao, Yoichiro Takada, Kentaro Omura and Shigeki Horiuchi	10
Strain localization and fabric development in polycrystalline anorthite + melt by water diffusion in an axial deformation experiment..... Jun-ichi Fukuda, Jun Muto and Hiroyuki Nagahama	10
In-situ permeability of fault zones estimated by hydraulic tests and continuous groundwater-pressure observations Norio Matsumoto and Norio Shigematsu	11
Complex microseismic activity and depth-dependent stress field changes in Wakayama, southwestern Japan Sumire Maeda, Toru Matsuzawa, Shinji Toda, Keisuke Yoshida and Hiroshi Katao	11
Interseismic crustal deformation in and around the Atotsugawa fault system, central Japan, detected by InSAR and GNSS..... Youichiro Takada, Takeshi Sagiya and Takuya Nishimura	12
Normal-faulting stress state associated with low differential stress in an overriding plate in northeast Japan prior to the 2011 Mw 9.0 Tohoku earthquake..... Makoto Otsubo, Ayumu Miyakawa and Kazutoshi Imanishi	12
Anelastic properties beneath the Niigata–Kobe Tectonic Zone, Japan..... Junichi Nakajima and Toru Matsuzawa	13
Spatial variation in coda Q in the northeastern part of Niigata–Kobe Tectonic Zone, central Japan: implication of the cause of a high strain rate zone..... Masanobu Dojo and Yoshihiro Hiramatsu	13
San-in shear zone in southwest Japan, revealed by GNSS observations..... Takuya Nishimura and Youichiro Takada	14
Sintering polycrystalline olivine and polycrystalline clinopyroxene containing trace amount of graphite from natural crystals..... Yumiko Tsubokawa and Masahiro Ishikawa	14